PHYSICAL REVIEW B **82**, 081415(R) (2010)

Anomalous anisotropy in athermal Bradley-Harper roughening of Cu(001)

Frank Everts, Herbert Wormeester, and Bene Poelsema
Solid State Physics, MESA+ Research Institute, University of Twente, P.O. Box 217, 7500 AE Enschede, The Netherlands
(Received 1 July 2010; published 27 August 2010)

Ion bombardment induced surface structures on Cu(001) have been studied under conditions obeying the previously "coined athermal Bradley-Harper (BH) region." Off-normal ion impact along the ⟨110⟩ and the ⟨100⟩ azimuth at 200 K gives rise to different high-resolution low-energy electron-diffraction patterns. Unanticipated and marked deviations from the inherent fourfold symmetry are obtained already at a polar angle of incidence as low as 10°. Experiments with 800 eV Ar^+ ions (flux 6×10^{12} ions cm^{-2} s^{-1} and fluence 4.3×10^{16} ions cm^{-2}) clearly show BH behavior for bombardment along [100] in contract to bombardment along [110]. This observation is attributed to the higher probability for surface penetration of ions when incident along ⟨100⟩. This remarkable finding is further corroborated by measurement at various energies between 0.2 and 2 keV along [100].

DOI: 10.1103/PhysRevB.82.081415 PACS number(s): 68.35.Fx, 81.16.Rf, 68.49.Sf, 61.05.jh

I. INTRODUCTION

Ion erosion has developed to a versatile technique for the preparation of nanostructures through self-organization. A milestone in the development of this technique for nanopatterning was the theoretical description of the process by Bradley and Harper (BH).[1] This approach predicts the formation of a ripple pattern as a result of an erosion instability. It explains that the ripple orientation is determined by the actual polar angle of incidence of the ions. For near normal incidence the ripples are oriented perpendicular to the plane of incidence of the ions while at a certain critical angle a crossover toward a parallel orientation for more oblique ion incidence angle is observed.[2] A basic ingredient for this description involves isotropic diffusion of species on the surface. Patterns created on single crystalline metal surfaces provide insight in the influence of diffusion on the pattern formation. Experiments on Cu and Ag(110) surfaces explore the influence of a strong anisotropic diffusion on these surfaces.[3,4] The patterns observed after normal-incidence sputtering on Cu(001) were explained with the differences in the so-called Ehrlich-Schwoebel (ES) barrier for interlayer diffusion, which attenuates the mass transport over the ⟨110⟩- and ⟨100⟩-oriented step edges[5] differently. It was found that as a result of this difference the etched morphology shows kinetically stabilized {103} facets at low substrate temperatures. In contrast, homoepitaxial growth leads to {113} facets at similar temperatures.[6] As suggested previously,[7] a strong postannealing effect of ion erosion induced structures on these (001) surfaces for temperatures above 250 K was observed.[5] Note that these facets are not the thermodynamically stable facets the word is generally referring to. In this Rapid Communication, we use the word facet for very well-defined "facetlike" features throughout.

The BH instability leads to ripple patterns observed on very different surfaces.[4,8,9] However, for temperatures below 400 K, a ripple pattern on both Cu and Ag(001) is only observed for grazing incidence sputtering.[10–12] As observed for normal-incidence sputtering,[5] the process leading to the etched structures is dominated by the ES barriers on these inherently isotropic surfaces. In their review, Chan and Chason[13] denoted this situation as the "ES instability" region. Ripple structures are also observed for higher ion fluxes and temperatures above 400 K and this region was denoted as the "BH instability" region. Above 400 K, the ES barrier associated with the ⟨110⟩ step edge [125 meV (Refs. 14 and 15)] no longer attenuates markedly the interlayer diffusion process. In the BH instability region also the characteristics of the BH instability, a change in ripple orientation with polar angle of incidence was observed for sputtering along the [100] azimuth. According to Chan and Chason, not only at high temperatures but also at low temperatures the influence of the ES barrier can be suppressed. This results in enhanced interlayer mass transport at low temperature.[16] For the (001) surfaces of Cu and Ag, this leads to the proposition of a so-called "athermal BH" region for temperatures below 200 K.[13] In this temperature regime, diffusion is limited but still active as observed from ripple formation at grazing incidence sputtering. The periodicity of the ripple pattern was shown to be linearly dependent on the ion energy. This dependence is the result of the short-lived thermal spike after ion impact.[12] This result showed that at low temperatures, the actual characteristics of the ion impact is much more pronounced in the observed pattern. In this Rapid Communication, we will show that a main characteristic of the BH instability, i.e., ripple rotation with polar angle of incidence is present in the athermal-BH region on the isotropic Cu(001) surface. Surprisingly, however, this is only observed for ion impact in the {100} plane, i.e., along the ⟨100⟩ azimuth and not for the ion impact in the {110} plane (along the ⟨110⟩ azimuth). Since in both cases the major part of the ion energy is transferred to the crystal, this difference must be solely attributed to the difference in penetration depth of the ions along the {110} plane and {100} plane. Highly surprisingly, already at very small angles of incidence this difference is very pronounced.

II. EXPERIMENTAL

The experiments were performed in an ultrahigh-vacuum chamber with a base pressure below 10^{-10} mbar. The Cu(001) crystal was cleaned with repeated sputter

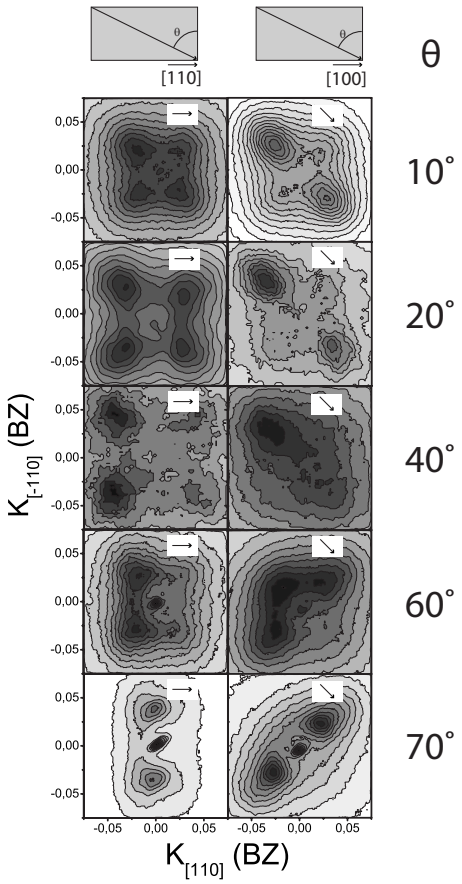

FIG. 1. HR-LEED measurements (contour plots of the intensity; arbitrary gray scales) at an electron energy of 275 eV after 2 h of sputtering at 200 K as a function of the polar angle of incidence from $\theta=10°$ to 70°. Shown are results for bombardment along the [110] (left) and [100] (right) directions of the Cu(001) surface. The ion energy was 800 eV and the ion current was 1 μA cm^{-2}, measured at normal incidence. The arrows indicate the azimuth direction of incidence.

(Ar^+,800 eV) anneal cycles.[10] The ion-induced patterns were created by sputtering with argon ions along either the [110] and [100] azimuth at a temperature of 200 K. After sputtering, the sample was rapidly cooled to below 130 K to avoid as much as possible postannealing effects. High-resolution electron-diffraction experiments were performed at this low temperature. For this purpose an Omicron spot profile analysis low-electron energy-diffraction (SPA-LEED) system was used. Electron-diffraction images were obtained for various electron energies to verify that features observed in the images were related to facets on the surface and to extract the actual facet orientation.

III. ANGLE OF INCIDENCE AND AZIMUTHAL DEPENDENCE

Figure 1 shows electron-diffraction images obtained for sputtering along both the [110] or [100] azimuth for various polar angles of incidence θ. All images were recorded after 2 h sputtering with 800 eV Ar ions on the Cu(001) surface held at a temperature of 200 K. At normal incidence, an ion current of 1 μA cm^{-2} is measured. The images for various angles of incidence obtained after sputtering along the [110] azimuth are very similar to previously reported results.[11] The patterns around normal incidence show a strictly fourfold-symmetric pattern with diffraction features along the [100] azimuth. These features represent the (103) facets associated with inverse pyramid structures created on this surface. The position of these features in reciprocal space varies with the electron energy.[5] For all images an electron energy of 275 eV was used (perpendicular phase $S_Z=4.91$).

Sputtering along the [100] azimuth results in very different electron-diffraction images. Already a polar angle of incidence of $\theta=10°$ is sufficient to break the fourfold-symmetry completely. This is in marked contrast with the result along the [110] azimuth. It is also remarkable that a small change in angle of incidence already results in such large differences. The two strong features in the azimuth direction of the sputter beam ([100]) indicate the formation of two well-defined (103) facets. For $\theta=10°$ only weak facet spots are observed in the direction perpendicular to the ion beam ([010]). A slight increase in the incidence angle to $\theta=20°$ virtually removes the intensity of these faint features. Only the two strong facet features in the direction parallel to the ion beam (see arrows) are observed. This indicates that a ripplelike structure perpendicular to the plane of the incident ion beam is created. The similar intensity of the two facet features changes around an incidence angle of $\theta=40°$ while for $\theta=60°$ a transition stage is observed. For $\theta=70°$ an electron image representative for a ripple structure parallel to the plane of the incident ion beam is observed. This change in ripple orientation with polar incidence angle for ion sputtering along the [100] azimuth is consistent with the main prediction of the BH theory, indicating a critical angle for orientation of around 60°. Ion bombardment along ⟨110⟩ leads to drastically different results. Only at grazing incidence ($\theta>70°$) ripples oriented parallel to ⟨110⟩ are formed. At smaller polar angles no ripple formation is detected and thus no evidence for BH behavior is present in the [110] data. Summarizing, an athermal-BH region in the sputter phase diagram for sputtering along the ⟨100⟩ azimuth is found.

To elucidate further the difference between sputtering along the two azimuth directions, the influence of the ion energy on the pattern formation for sputtering along the [100] azimuth was investigated. Figure 2(a) shows the SPA-LEED measurements after sputtering at $\theta=20°$ with an ion energy of 200 and 800 eV. For $\theta=20°$ faint side peaks of the broken fourfold symmetry are visible, which makes it easier to identify the influence of the decrease in ion energy. The much lower flux of the ion gun at 200 eV (0.55×10^{12} ions cm^{-2} s^{-1}) was compensated by sputtering for 22 h, leading to the same fluence as for the data displayed in Fig. 1. These low ion flux results illustrate that the ion energy indeed strongly influences the symmetry of the observed diffraction pattern. The result obtained with 800 eV ions also shows pronounced features in the [100] direction. In contrast to the higher flux situation at this polar angle of incidence (see Fig. 1) weaker features in the direction perpendicular to the plane of the incident ion beam, i.e., along $[1\bar{1}0]$ can be distinguished. This shows resemblance to the observation for

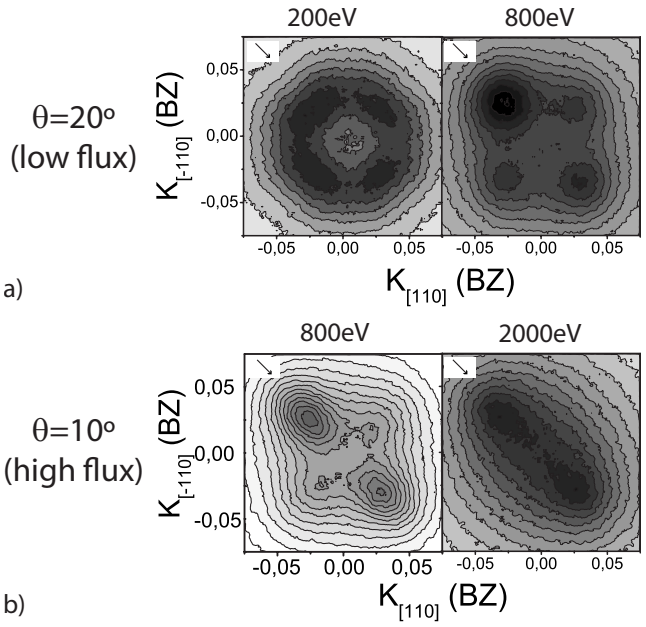

FIG. 2. HR-LEED measurements at an electron energy of 275 eV after Ar ion bombardment at a temperature of 200 K along the [100] azimuth. (a) Sputtering at $\theta=20°$ for 22 h with a flux of 0.55×10^{12} ions cm^{-2} s^{-1}. The ion energies are 200 eV and 800 eV, respectively. (b) Sputtering with $\theta=10°$ for 2 h with a flux of 6×10^{12} ions cm^{-2} s^{-1}. The energies are 800 eV and 2 keV, respectively.

$\theta=10°$ in Fig. 2(b). The sputtering at 200 eV results in a very different pattern, showing a fourfold symmetry akin to those obtained for sputtering at normal incidence or at near normal incidence along the [110] azimuth. The facet features are less pronounced and actually instead of four facet peaks eight features may be discerned. The latter is probably the result of the smaller interlayer mass transport experienced for the extended sputter time. In this situation a tendency to strive for the more energetically favorable ⟨110⟩ step edges is expected[5] and a mixed situation results. The presence of the fourfold symmetry after sputtering with 200 eV energy ions shows that the details of the ion impact, in particular the ion energy, determine the pattern formation in the athermal-BH region.

Figure 2(b) shows the diffraction images for sputtering at $\theta=10°$ along the [100] azimuth with ion energies of 800 eV and 2 keV. Again, the faint side peaks of the broken fourfold symmetry are visible, which makes it easier to identify the influence of the increase in ion energy. The diffraction image after sputtering at 800 eV shows both prominent facet features along [100] and very weak features along [010]. An increase of the ion energy to 2 keV results in a total vanishing of the weak features, leading to an even more anisotropic morphology.

The results shown in Figs. 1 and 2 illustrate that the details of ion impact itself play a crucial role as evidenced by the different degree of anisotropy in the diffraction patterns. The angle of incidence (both polar and azimuth) as well as the ion energy, and thus the penetration depth of the ion into the crystal, determine the details of this ion impact. The differences observed in the data in Fig. 1 obtained after sputtering with the same ion energy of 800 eV and the same polar angle of incidence show that the azimuth angle has a profound influence, related to sputtering along the ⟨110⟩ and ⟨100⟩ azimuth.

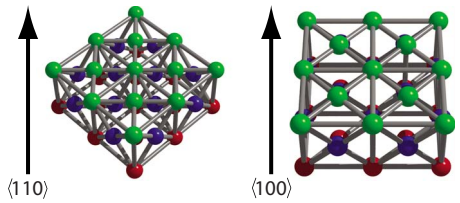

FIG. 3. (Color online) Crystallographic orientations of the fcc(001) crystal at a viewing angle of 20°. The top layer is indicated with green (gray). The second and third layers are indicated with blue and red (black), respectively (see text).

There is a huge difference in sputter efficiency for (near) normal-incidence sputtering along the two azimuthal directions. This is directly related to the penetration of the ions in the crystal and thus the possibility to reach deeper layers. Channeling is the easiest way to achieve this. At near normal incidence, there is channeling possible for both azimuthal directions. Obviously, along the ⟨110⟩ azimuthal direction planar channeling is possible in the {110} plane and along the ⟨100⟩ azimuthal direction planar channeling is possible in the {100} plane. Although at first sight these planar channels look equivalent, this is not the case (Fig. 3). Since the distance between atoms along the ⟨110⟩ azimuth is smaller (1.28 Å) than along the ⟨100⟩ direction (1.81 Å), the distance between the {110} planes is also smaller than the distance between the {100} planes. Therefore, planar channeling close to normal incidence will be much easier along the ⟨100⟩ direction, which enhances the sputter efficiency dramatically.

Not only at near normal incidence but also for increasing polar angle channeling can occur. For sputtering along the ⟨110⟩ azimuth there is a {111} planar channel at an angle of 35.3° accessed. With the interlayer distance of 2.55 Å the probability for penetrating more deeply into the crystal becomes relatively high. For sputtering along the ⟨100⟩ azimuth, at an angle of 45° with the surface normal, there is an axial channel along the ⟨101⟩ direction. In both cases this is the polar angle where a transition in diffraction pattern was observed.

IV. SUMMARY

Surprisingly, the azimuthal orientation was found to play already a prominent role on the etch pattern formation for near normal incident ion bombardment on Cu(001) with 800 eV Ar^+ ions. A profound difference in the symmetry of the electron-diffraction pattern is observed for a polar angle of incidence of only 10° between sputtering along the [110] and the [100] azimuth. In contrast, bombardment along the [110] azimuth shows a gradual transition from the fourfold-symmetric diffraction pattern as observed for normal-incidence sputtering to a twofold-symmetric diffraction pattern observed for oblique incident sputtering. Bombardment along the [100] azimuth shows already for near normal

incidence a twofold-symmetry pattern. The orientation of the ripples associated with this pattern rotates from perpendicular to the ion beam to parallel to the ion beam with increasing ion incidence angle. This behavior is expected within the Bradley-Harper description of ion beam induced roughening. The remarkable difference in behavior for sputtering along the ⟨110⟩ and ⟨100⟩ azimuth is solely caused by a difference in penetration depth of the incoming ion due to the screening by atoms in the outermost layer. Experiments with different ion energies verify the pronounced influence of the penetration depth on the development of the surface morphology.

ACKNOWLEDGMENTS

F.E. and H.W. acknowledge the fruitful discussions with G. Castro from the SpLine BM25 beamline at the ESRF. This research is supported by NanoNed, a national nanotechnology program coordinated by the Dutch Ministry of Economic Affairs.

[1] R. M. Bradley and J. M. E. Harper, J. Vac. Sci. Technol. A **6**, 2390 (1988).
[2] H. Hansen, A. Redinger, S. Messlinger, G. Stoian, Y. Rosandi, H. M. Urbassek, U. Linke, and T. Michely, Phys. Rev. B **73**, 235414 (2006).
[3] S. Rusponi, G. Costantini, C. Boragno, and U. Valbusa, Phys. Rev. Lett. **81**, 4184 (1998).
[4] U. Valbusa, C. Boragno, and F. Buatier de Mongeot, J. Phys.: Condens. Matter **14**, 8153 (2002).
[5] P. Broekmann, A. Mewe, H. Wormeester, and B. Poelsema, Phys. Rev. Lett. **89**, 146102 (2002).
[6] L. C. Jorritsma, M. Bijnagte, G. Rosenfeld, and B. Poelsema, Phys. Rev. Lett. **78**, 911 (1997).
[7] C. Teichert, C. Ammer, and M. Klaua, Phys. Status Solidi A **146**, 223 (1994).
[8] J. Erlebacher, M. J. Aziz, E. Chason, M. B. Sinclair, and J. A. Floro, Phys. Rev. Lett. **82**, 2330 (1999).
[9] S. Habenicht, W. Bolse, K. P. Lieb, K. Reimann, and U. Geyer, Phys. Rev. B **60**, R2200 (1999).
[10] F. Everts, H. Wormeester, and B. Poelsema, Phys. Rev. B **78**, 155419 (2008).
[11] H. Wormeester and B. Poelsema, J. Phys.: Condens. Matter **21**, 224002 (2009).
[12] S. van Dijken, D. de Bruin, and B. Poelsema, Phys. Rev. Lett. **86**, 4608 (2001).
[13] W. L. Chan and E. Chason, J. Appl. Phys. **101**, 121301 (2007).
[14] R. Gerlach, T. Maroutian, L. Douillard, D. Martinotti, and H.-J. Ernst, Surf. Sci., **480**, 97 (2001).
[15] F. L. W. Rabbering, H. Wormeester, F. Everts, and B. Poelsema, Phys. Rev. B **79**, 075402 (2009).
[16] R. Kunkel, B. Poelsema, L. K. Verheij, and G. Comsa, Phys. Rev. Lett. **65**, 733 (1990).